

Received March 19, 2021, accepted April 5, 2021, date of publication April 20, 2021, date of current version May 5, 2021.

Digital Object Identifier 10.1109/ACCESS.2021.3074381

A Unified SO(3) Approach to the Attitude Control Design for Quadrotors

JEN-TE YU^{ID}

Department of Electrical Engineering, Chung Yuan Christian University, Taoyuan City 32023, Taiwan

e-mail: yu@cyu.edu.tw

This work was supported by the Ministry of Science and Technology of Taiwan under Grant MOST108-2221-E-033-046.

ABSTRACT This paper proposes a two-phased problem reformulation approach to solve the quadrotor UAV attitude control problem. Given an initial attitude, the objective is to design a control to drive it toward a desired value. The first phase begins with the definition of three types of errors pertaining to attitude discrepancy, followed by the utilization of virtual control with which the dynamics of quadrotor's attitude and angular velocity are then unified under the framework of SO(3), rendering the original control problem much more transparent to tackle. Through cancellation of certain unwanted terms emerging from the unification process, entry-wise treatment of the remaining matrix dynamics is then employed in the second phase to transform it further into the stabilization problem of a 3-dimensional linear time-invariant system that is fairly easy to solve since to which standard feedback designs such as linear quadratic regulator and pole placement are readily applicable. In addition to the classical designs, a specialized and structurally simple controller is provided to reduce the number of gains. To account for system parametric uncertainties, external disturbances, and sensor measurement errors and noises, a second controller based on classical H_{∞} theory is presented to enhance the robustness of the design. A numerical example is given, and computer simulations are conducted to generate error and control trajectories to assess and compare the effectiveness of the presented designs.

INDEX TERMS Quadrotor UAV, attitude, rotation matrix, special orthogonal group SO(3), virtual control, entry-wise stabilization, linear quadratic regulator, pole placement, disturbance attenuation, H_{∞} control.

I. INTRODUCTION

Over the past three decades, the unmanned aerial vehicles (UAVs) have been a subject of considerable attention. The quadrotor UAV (quadrotor for short in the sequel) is rapidly growing in popularity and attracts great interest from various sectors thanks to its great advantages including vertical taking off and landing, and rapid maneuvering. Typical applications include spraying pesticide and fertilizer, delivering goods, surveillance, monitoring, patrolling, fire-fighting, aerial mappings, detecting incidents, taking photo pictures/video recording, to name just a few [1].

The dynamics of quadrotor exhibits under-actuation and strongly coupling natures, which can be classified into two types – the translational motion and the rotational motion. The former includes changes of altitude, linear speed and acceleration, and is referred to as the outer loop, whereas the latter studies changes of attitude including attitude angles and

The associate editor coordinating the review of this manuscript and approving it for publication was Fangfei Li^{ID}.

angular velocities, and is referred to as the inner loop. See Fig. 1 for a schematic of the rotational motion of a quadrotor.

With high potential in various fields, its operation and maintenance costs and risks are relatively low, extensive new applications are expected to appear in the near future; therefore the research on the quadrotors is important [1].

It is worth noting that the translational motion depends on the rotational motion, but the converse does not hold. As such, the attitude control can be designed separately and independently. Even so, some existing works go one step further and deal with both translational and rotational motions at the same time, such as Zhao *et al.* [4], Shi *et al.* [7], and García *et al.* [12], Nikhilraj *et al.* [14], and Izaguirre-Espinosa *et al.* [15]. This paper focuses its study on the second type of motion. Specifically, the goal is to design a controller that makes the quadrotor track a desired and predetermined attitude.

Parametric uncertainties may exist in practice, such as mass and/or moment of inertia of the quadrotor and often-times adaptive controllers are utilized to deal with them, see,

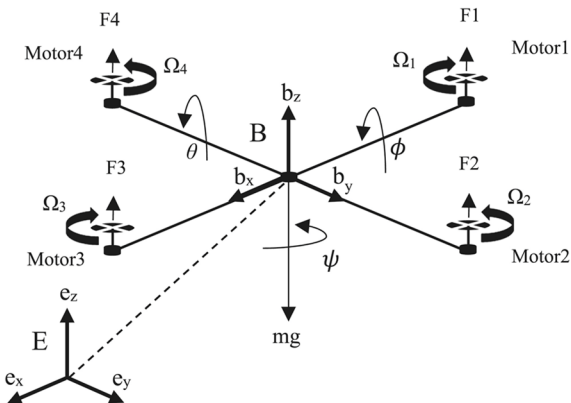


FIGURE 1. A schematic of rotational motion of quadrotor with body and earth reference frames. (source: <https://doi.org/10.1002/asjc.1758>).

for example, Lee [3], Zhao *et al.* [4], Bhatia *et al.* [11], García *et al.* [12], and Chu *et al.* [17]. Some authors also addressed the issue of external disturbances and/or uncertain system dynamics with robust control designs including Lee [3], Zhao *et al.* [4], Lee [6], Tian *et al.* [8], Jiang *et al.* [9], Bhatia *et al.* [11], García *et al.* [12], Tian *et al.* [13], Izaguirre-Espinosa *et al.* [15], and Chu *et al.* [17]. Among them, Tian *et al.* [8], García *et al.* [12], Tian *et al.* [13], and Izaguirre-Espinosa *et al.* [15] used sliding mode control.

Super-twisting attitude control algorithms and the-like were proposed by Tian *et al.* [8], Jiang *et al.* [9], and Tian *et al.* [13] to suppress chattering wherein a discontinuous integral control was added in Tian *et al.* [8] to account for the matched disturbances but a disturbance observer was employed instead in Jiang *et al.* [9].

Some critical applications such as emergency and military operations may require finite time convergence as presented in Shi *et al.* [7], Tian *et al.* [8], Jiang *et al.* [9], García *et al.* [12], Tian *et al.* [13], and Izaguirre-Espinosa *et al.* [15] with the latter using fractional-order controller and model-free position tracking scheme.

As a space representing rigid-body rotations and free of gimbal lock and unwinding phenomenon, the special orthogonal group SO(3) is a Lie group that has an algebraic structure in the operation of matrix multiplication and a differential geometric structure – a compact and smooth manifold that facilitates the use of calculus [2]. In addition, it features global attitude definition and one-to-one mapping [2].

SO(3) was utilized by Lee [3], Berkane *et al.* [10], Akhtar *et al.* [16], and Tan *et al.* [18] to design their attitude controllers, and among them Berkane *et al.* [10] relied only on attitude information using an angular velocity observer while Tan *et al.* [18] employed an overlapping cell-like sampling on SO(3) to build a graph model on which a search algorithm was constructed to generate a feasible path. As opposed to SO(3), the Special Euclidean space SE(3) was used in Nikhilraj *et al.* [14] to represent the attitude and an energy-optimal trajectory generation scheme was presented to drive the quadrotor to the desired state. Since there are only a few results in the literature [3], [10], [16], [18], it is

important to further explore SO(3) on the quadrotor research due to its appealing properties mentioned above. As such, SO(3) is adopted by this paper as a framework to unify the two dynamic equations pertaining to the quadrotor's rotational motion and its control.

Backstepping/virtual control is a widely used method, see, for example, Choi and Ahn [5], Jiang *et al.* [9], Bhatia *et al.* [11], García *et al.* [12], and Izaguirre-Espinosa *et al.* [15]. The mature technique will be utilized as well in this study to begin the design procedure.

The contribution of this paper is that it proposes a two-phased transformation process to unify the attitude dynamics under the SO(3) framework and linearize the attitude control system. Compared with other methods, the advantages of the proposed approach include: the problem is made much more transparent to tackle, the controller becomes much more straightforward to design, and the dimension of the problem is reduced to be much lower making many classical control schemes readily applicable. The design procedure is outlined below.

Firstly, for control purpose, three types of errors are defined. Upon consideration of the error dynamics, virtual control is employed to regulate the attitude error to zero. Secondly, the dynamics of the quadrotor's attitude and angular velocity are unified under the SO(3) framework with the aid of three algebraic facts. The choice of the first component of control emerges in a natural manner at this point, as it can be used to cancel some unwanted terms appearing in the error dynamics. An important result out of this cancellation is that the remaining matrix error dynamics, when treated entry-wise, becomes a three-dimensional linear time-invariant (LTI) system. Stabilization of such low dimensional LTI systems using static (constant) feedback gain can be easily achieved by classical control schemes, provided no uncertainties and/or disturbances exist. Finally, to address the system parametric uncertainties, external disturbances, and sensor measurement errors and noises, a second static design is presented that is based on classical H_∞ control theory making the proposed scheme more robust and practical.

The rest of the paper is organized as follows. The system considered in this paper is given in Section II, where the dynamic model, basic assumptions, and objectives are presented. Also introduced in this section are properties of the rotation matrices and the skew-symmetrification operation of vectors and its inverse operation. In Section III, a virtual control is used to begin the design. Also defined in the same section for controller design purpose are three types of errors – integral attitude error, proportional attitude error, and control error. Aided by three facts, the original attitude control problem is reformulated in Section IV wherein both the dynamics of the angular velocity and the control are skew-symmetrified under a unified SO(3) framework leading to the choice for the first component of the control. The stabilization of a 3-dimensional LTI system is also shown to emerge naturally as the remaining dynamics to be controlled, provided the stabilization of the differential

matrix error dynamics are treated entry-wise. Under zero disturbance/uncertainty assumption, Section V addresses the choice of the feedback gain of the LTI system and offers two designs for the nominal system – linear quadratic regulator (LQR) and a specialized one. Using classical robust control techniques, Section VI presents a static attitude control design in the H_∞ sense equipping the control system with disturbance attenuation capabilities. Section VII discusses the stability type of the closed loop system. A numerical example is provided in Section VIII to validate the new approach. Also presented in this section are trajectories of errors, angular velocities, and controls for performance assessment purpose. Future works and challenges are discussed in the conclusion as Section IX.

Throughout the paper, vector ω stands for the angular velocity of the quadrotor, R refers to the rotation matrix associated with a set of Euler angles that represents an attitude, E stands for attitude error, I_R refers to integral of error associated with rotation matrix, Δ and d represent lumped disturbances and/or uncertainties, γ stands for disturbance attenuation level, I_3 is an identity matrix of dimension 3, \hat{a} and $(\bullet)^\wedge$ refer to a skew-symmetric matrix pertaining to vector a , and vector (\bullet) , respectively, eigenvalue is denoted as λ , moment of inertia is represented by J , *Cofactor*(J) refers to the cofactor matrix of J , which is also shortened as *Cof*(J), $|J|$ refers to determinant of J , and $\|\cdot\|$ stands for matrix norm or vector length. For a matrix M , the inequality $M < 0$ means it is negative definite, and *Det*(M) stands for its determinant.

II. THE SYSTEM MODEL AND CONTROL OBJECTIVES

Given in Fig. 1 is a schematic of the rotational motion of quadrotor under study. Specifically, the attitude dynamics of the quadrotor is mathematically expressed as follows

$$J\dot{\omega} = (J\omega) \times \omega + u + \Delta, \quad J = \begin{bmatrix} J_1 & 0 & 0 \\ 0 & J_2 & 0 \\ 0 & 0 & J_3 \end{bmatrix}, \quad (1)$$

$$\begin{aligned} \omega &\in \mathfrak{R}^3, \quad u \in \mathfrak{R}^3, \quad \Delta \in \mathfrak{R}^3 \\ \dot{R} &= R\hat{\omega}, \quad R \in \mathfrak{R}^{3 \times 3}, \quad \hat{\omega} \in \mathfrak{R}^{3 \times 3} \end{aligned} \quad (2)$$

where ω is the angular velocity, J is the moment of inertia, which, under normal circumstances, is diagonal due to the symmetrical structure of the quadrotor UAV, u is the control to be designed, R is the rotation matrix that is orthonormal and Δ stands for lumped uncertainties and disturbances.

Note that matrix $\hat{\omega}$ can be viewed as the skew-symmetrified counterpart of the velocity vector ω defined as

$$\omega = \begin{bmatrix} \omega_1 \\ \omega_2 \\ \omega_3 \end{bmatrix}, \quad \hat{\omega} = \begin{bmatrix} 0 & -\omega_3 & \omega_2 \\ \omega_3 & 0 & -\omega_1 \\ -\omega_2 & \omega_1 & 0 \end{bmatrix} \quad (3)$$

$$R^T R = R R^T = I_3, \quad \hat{\omega}^T = -\hat{\omega} \quad (4)$$

As will be seen later, the operation and the reverse operation of skew-symmetrification play an important role in the control design.

The desired rotation matrix must be admissible in the first place in the sense that it is orthonormal satisfying

$$R_d^T R_d = R_d R_d^T = I_3. \quad (5)$$

Without loss of generality, this paper focuses on the case where the desired rotation matrix R_d is constant. Equivalently, given an admissible initial rotation matrix R , the goal is to make it approach R_d using the control u . They come directly from the roll, pitch, and yaw angles that define the attitude of a quadrotor UAV.

III. THREE TYPES OF ERRORS AND VIRTUAL CONTROL

The attitude of a quadrotor, in general, is defined by a set of 3D Euler angles – the so-called roll, pitch, and yaw angles (denoted as ϕ , θ and ψ , respectively in this paper). Associated with this set of Euler angles is a rotation matrix resulting from a body-fixed axis rotation sequence that corresponds to the given set of Euler angles. The attitude error in the form of Euler angles is equivalent to the attitude error in the form of rotation matrix that is adopted in this paper.

Given two admissible matrices R and R_d , the objective is to design the control u to drive the discrepancy between the two to zero. The design is composed of two phases and corresponding to which there will be two different sets of gains to be determined, which will be detailed shortly.

We begin the first phase of design by defining an error on the rotation matrix

$$E_R = R - R_d \quad (6)$$

which is to be driven to zero. Given the above expression and equation (2), one may have

$$\dot{E}_R = \dot{R} - \dot{R}_d = R\hat{\omega} \quad (7)$$

If matrix $R\hat{\omega}$ were the control, it may be chosen to drive the attitude error to zero. Without loss of generality, suppose

$$(R\hat{\omega})_{vir} = -g_p E_R, \quad g_p > 0 \quad (8)$$

where the subscript “vir” stands for virtual and g_p is a positive scalar proportional gain at our disposal. To reduce steady-state error, an integral control may be added, which is defined as

$$I_R = \int_0^t E_R(\tau) d\tau \quad (9)$$

With this integral term, the virtual control is re-defined as

$$(R\hat{\omega})_{vir} = g_i I_R - g_p E_R, \quad 0 < |g_i| \ll 1 \quad (10)$$

where g_i is a scalar integral gain at our disposal as well. Under normal circumstances, small g_i suffices.

Apparently, discrepancy exists between the virtual control and its actual value hence another error may be defined as

$$E_\omega = R\hat{\omega} - (R\hat{\omega})_{vir} = R\hat{\omega} - g_i I_R + g_p E_R \quad (11)$$

IV. PROBLEM REFORMULATION UNDER A UNIFIED SO(3) FRAMEWORK AND ENTRY-WISE STABILIZATION

The second phase of design is presented in this section. The problem reformulation process consists of several steps including: utilization of three algebraic facts to facilitate the skew-symmetrification operation; entry-wise treatment of the remaining dynamics after cancelation of unwanted terms that leads to the desired linearization and dimension reduction rendering many classical control designs readily applicable. Note that the dynamics of the angular velocity can be rewritten as

$$\dot{\omega} = J^{-1}[(J\omega) \times \omega + u + \Delta]. \quad (12)$$

Since the two dynamic equations (1)-(2) are coupled, for consistency, the design will be performed on the dynamics of $\hat{\omega}$ instead of ω . That is, the system dynamics will be unified under the framework of SO(3). To that end, three important facts are needed hence provided below where a and b are any 3-dimensional vectors, D is any 3×3 matrix, $(a \times b)^{\wedge}$ refer to a skew-symmetric matrix pertaining to vector $(a \times b)$, Cof stands for cofactor, and $|J|$ represents determinant of J .

- Fact 1* : $(Da) \times (Db) = Cof(D)(a \times b)$,
 - Fact 2* : $(a \times b)^{\wedge} = ba^T - ab^T$,
 - Fact 3* : $J^{-1} = |J|^{-1}Cof(J)$.
- (13)

Based on these three facts, the dynamics of angular velocity can be rewritten as

$$\dot{\omega} = |J|^{-1} \left[(J^2 \omega) \times (J\omega) \right] + J^{-1}u + J^{-1}\Delta, \quad (14)$$

where $J^{-1}u$ takes the form

$$J^{-1}u = \begin{bmatrix} J_1^{-1}u_1 \\ J_2^{-1}u_2 \\ J_3^{-1}u_3 \end{bmatrix}. \quad (15)$$

Now the skew-symmetrified counterpart of the angular velocity dynamics, as a direct result of Fact 2 given above, reads

$$\dot{\hat{\omega}} = |J|^{-1} \left[J\omega\omega^T J^2 - J^2\omega\omega^T J \right] + (J^{-1}u)^{\wedge} + (J^{-1}\Delta)^{\wedge} \quad (16)$$

with the control assuming the form

$$(J^{-1}u)^{\wedge} = \begin{bmatrix} J_1^{-1}u_1 \\ J_2^{-1}u_2 \\ J_3^{-1}u_3 \end{bmatrix}^{\wedge} = \begin{bmatrix} 0 & -J_3^{-1}u_3 & J_2^{-1}u_2 \\ J_3^{-1}u_3 & 0 & -J_1^{-1}u_1 \\ -J_2^{-1}u_2 & J_1^{-1}u_1 & 0 \end{bmatrix} \quad (17)$$

Next, substitute (2) and (16) into the dynamics of E_{ω}

$$\begin{aligned} \dot{E}_{\omega} &= \dot{R}\hat{\omega} + R\dot{\hat{\omega}} - g_i E_R + g_p \dot{E}_R \\ &= R\hat{\omega}^2 + |J|^{-1}R \left(J\omega\omega^T J^2 - J^2\omega\omega^T J \right) \\ &\quad - g_i E_R + g_p \dot{E}_R + R \left(J^{-1}u \right)^{\wedge} + R \left(J^{-1}\Delta \right)^{\wedge}. \end{aligned} \quad (18)$$

Suppose the control is divided into two parts (subscripted by 1 and 2, respectively) with the first of which canceling the unwanted nonlinear terms in (18)

$$\begin{aligned} \left(J^{-1}u \right)^{\wedge} &= \left(J^{-1}u \right)_1^{\wedge} + \left(J^{-1}u \right)_2^{\wedge} \\ \left(J^{-1}u \right)_1^{\wedge} &= |J|^{-1} \left(J^2\omega\omega^T J - J\omega\omega^T J^2 \right) - \hat{\omega}^2. \end{aligned} \quad (19)$$

For convenience, define F as

$$F = R \left(J^{-1}u \right)_2^{\wedge}. \quad (20)$$

It could be, for simplicity, chosen to be linear as

$$F = -(k_i I_R + k_p E_R + k_{\omega} E_{\omega}), \quad (21)$$

where the scalars k_i , k_p and k_{ω} belong to the second set of gains to be designed. The second control component can be obtained easily as

$$\left(J^{-1}u \right)_2^{\wedge} = R^T F = -R^T (k_i I_R + k_p E_R + k_{\omega} E_{\omega}). \quad (22)$$

Putting the two control components together one gets

$$\begin{aligned} \left(J^{-1}u \right)^{\wedge} &= |J|^{-1} \left(J^2\omega\omega^T J - J\omega\omega^T J^2 \right) - \hat{\omega}^2 \\ &\quad - R^T (k_i I_R + k_p E_R + k_{\omega} E_{\omega}). \end{aligned} \quad (23)$$

As the proposed control uses data of attitude and angular velocity that are measurement based, sensor errors and noises will have some impact on the result in practice. Without loss of generality, such practical factors can be incorporated into Δ of (1) that stands for lumped uncertainties and disturbances, although they are different in nature.

The remaining error dynamics now become

$$\dot{I}_R = E_R, \quad (24)$$

$$\dot{E}_R = g_i I_R - g_p E_R + E_{\omega}, \quad (25)$$

$$\begin{aligned} \dot{E}_{\omega} &= (g_i g_p - k_i) I_R - (g_i + g_p^2 + k_p) E_R + (g_p - k_{\omega}) E_{\omega} \\ &\quad + R \left(J^{-1}\Delta \right)^{\wedge}. \end{aligned} \quad (26)$$

Note that (24)-(26) is a system of linear first order differential matrix equations with constant coefficients. If they are treated entry-wise, a 3-dimensional linear time-invariant (LTI) system naturally arises

$$\begin{aligned} \dot{e} &= Ae + Bf + Bd \\ e &= [e_I \ e_R \ e_{\omega}]^T \in \mathfrak{R}^3, \quad d \in \mathfrak{R}, f \in \mathfrak{R}, \end{aligned} \quad (27)$$

where the variable e_I refers to a corresponding entry of the error matrix I_R , the variable e_R refers to a corresponding entry of the error matrix E_R , the variable e_{ω} refers to a corresponding entry of the error matrix E_{ω} , respectively and the scalar control f in fact is the entry-wise counterpart of F that should be chosen to stabilize this LTI system, and d refers to an entry of the matrix pertaining to the lumped disturbances and/or

uncertainties in (26). The open loop matrix A and matrix B in (27) are given as follows

$$A = \begin{bmatrix} 0 & 1 & 0 \\ g_i & -g_p & 1 \\ g_i g_p & -g_i - g_p^2 & g_p \end{bmatrix}, \quad B = \begin{bmatrix} 0 \\ 0 \\ 1 \end{bmatrix} \quad (28)$$

As assumed in (21), the scalar control f takes the state feedback form

$$f = -Ke, \quad K = [k_i \quad k_p \quad k_\omega] \in \mathbb{R}^{1 \times 3} \quad (29)$$

See Fig. 2 for a schematic diagram for the structure of the proposed control system. The design of the three scalar gains is discussed next.

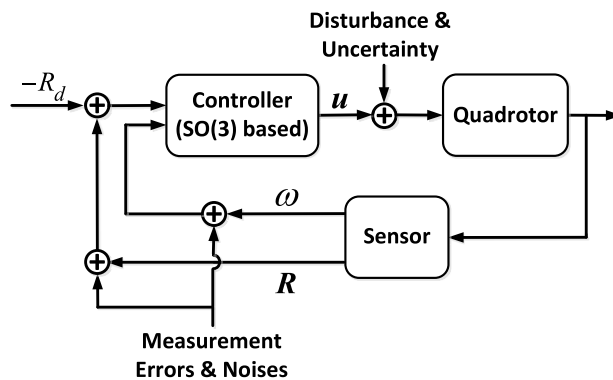


FIGURE 2. A schematic diagram for the structure of the proposed control system.

V. THE GAIN DESIGN OF THE NOMINAL SYSTEM

Up to this point, the choice of the stabilizing state feedback gain K has not been addressed yet. The details are provided in the present and next sections. As for implementation, one just needs to use (17) and (23) to recover the actual control.

There are plentiful standard designs that are readily applicable to determine the gains of the nominal system such as classical LQR and pole placement methods. For easy exposition, only the classical LQR design and a specialized one are presented.

A. STANDARD LQR DESIGN

The Linear Quadratic Regulator (LQR) design takes the form

$$K = [k_i \quad k_p \quad k_\omega] = B^T P, \quad (30)$$

$$A^T P + PA - PBB^T P + I = 0, \quad P = P^T > 0. \quad (31)$$

Equation (31) is the well-known continuous-time algebraic Riccati equation. For simplicity, the two weighting matrices in the LQR are chosen to be the identity matrix [19].

Note that matrix P is symmetric and positive definite and the resultant closed loop matrix can be written as

$$A_c = \begin{bmatrix} 0 & 1 & 0 \\ g_i & -g_p & 1 \\ g_i g_p - k_i & -g_i - g_p^2 - k_p & g_p - k_\omega \end{bmatrix}. \quad (32)$$

Remarks: The convergence speed of the proposed control algorithm can be controlled by the selection of the feedback gain K of (30) in terms of its numeric values. For example, smaller control weighting in the LQR design in general will give rise to a larger gain, which in turn will lead to a higher convergence speed. The reader is referred to [19] for more technical details. However, the use of a larger gain in the meantime implies more control energy is put into the system, which inevitably costs more in some sense. As such, there is a trade-off between the two, apparently. One of the reasons LQR design is introduced to the proposed framework is that it explicitly defines a cost function (a quadratic sum of the state and the control) that is used as a measure to evaluate the overall performance (hence the so-called state cost and control cost [19]).

B. A SPECIALIZED DESIGN

Besides the standard LQR and pole placement schemes, an interesting gain design is presented below that feeds back E_ω only. Given below are two facts about the closed loop eigenvalues

$$\text{Trace}(A_c) = \sum_{i=1}^3 \lambda_i(A_c) = -k_\omega, \quad (33)$$

$$\text{Det}(A_c) = \prod_{i=1}^3 \lambda_i(A_c) = g_i k_\omega - k_i. \quad (34)$$

Apparently, the following expressions must hold

$$0 < k_\omega, \quad g_i k_\omega < k_i. \quad (35)$$

We may choose $g_i < 0, k_i = 0, k_p = 0$, and obtain

$$K = [0 \ 0 \ k_\omega], \quad (36)$$

$$\hat{v}_2 = R^T F = -k_\omega R^T E_\omega. \quad (37)$$

The number of gains used by \hat{v}_2 in this specialized scheme is reduced from three to one, as can be seen from the following

$$A_c = \begin{bmatrix} 0 & 1 & 0 \\ g_i & -g_p & 1 \\ g_i g_p - k_i & -g_i - g_p^2 - k_p & g_p - k_\omega \end{bmatrix}. \quad (38)$$

An illustrative numerical example will be given in a later section that employs this specialized design.

VI. CLASSICAL ROBUST CONTROL DESIGN

Standard H_∞ robust control is presented in this section to explicitly account for the uncertainties and/or external disturbances in the controller design. Given below is taken from Green and Limebeer [20] in which η stands for performance output at our disposal, γ refers to prescribed disturbance attenuation level, and both A_c and $A_{c\gamma}$ are asymptotically stable

$$\dot{e} = Ae + Bf + Bd, \quad f = -Ke, \quad K = B^T P, \quad \eta = \begin{bmatrix} e \\ f \end{bmatrix}, \quad (39)$$

$$A^T P + PA - \left(1 - \gamma^{-2}\right) PBB^T P + I = 0, \quad (40)$$

$$A_c = A - BK, A_{c\gamma} = A - \left(1 - \gamma^{-2}\right) BK. \quad (41)$$

In terms of its infinity norm (which is the maximum induced 2-norm) [20], the transfer function from the disturbance d to the performance output η is guaranteed to fall below the prescribed value γ , provided the feedback gain K in (39) is employed. To be more specific, the following holds

$$\|G_{\eta d}(s)\|_\infty < \gamma. \quad (42)$$

The disturbance attenuation level γ must be chosen as such that the *Hamiltonian matrix* H has no imaginary axis eigenvalue [20] where matrix H takes the form

$$H = \begin{bmatrix} A - BK & \gamma^{-2} BB^T \\ \begin{bmatrix} I \\ -K \end{bmatrix} & -(A - BK)^T \end{bmatrix}. \quad (43)$$

Apparently, the condition of no imaginary eigenvalue will be violated if γ is too small [20]. The derivation and proof are omitted here and the reader is referred to [20] for further technical details.

Note that equation (40) can be rewritten in the following form

$$A_{c\gamma}^T P + PA_{c\gamma} - \gamma^{-2} PBB^T P + I + PBB^T P = 0 \quad (44)$$

Given below is a part of a heuristic iterative algorithm that can be used to solve (44) for P where the subscript “ j ” stands for index of iteration

$$\begin{aligned} A_{c\gamma j}^T P_{j+1} + P_{j+1} A_{c\gamma j} - \gamma^{-2} P_{j+1} BB^T P_{j+1} \\ + I + P_j BB^T P_j = 0 \end{aligned} \quad (45)$$

Equation (45) is more like a standard Riccati equation [19]. We will not go further in this direction as it is beyond the scope of current study.

Remarks: In addition to those sliding-mode controls reviewed in Section I, there exist many more literatures that utilize such kind of schemes to deal with disturbances. See, for example, recent accounts [21]–[23]. Ideally, these control algorithms should perform better than the H_∞ design presented above, but the trade-off apparently is that they are computationally much more demanding/costly due to their structural complexities. Unlike the proposed static H_∞ design, those sliding-mode controllers and the-like are dynamic, hence are more involved from the implementation point of view.

VII. STABILITY OF CLOSED LOOP SYSTEM

Closed loop stability is analyzed in this section. Recall treating the error dynamics entry-wise we were able to obtain a 3-dimensional LTI system in which matrix K may be any stabilizing state feedback gain. Rewrite the closed-loop error dynamics as

$$\dot{e} = A_c e + Bd, \quad A_c = A - BK \quad (46)$$

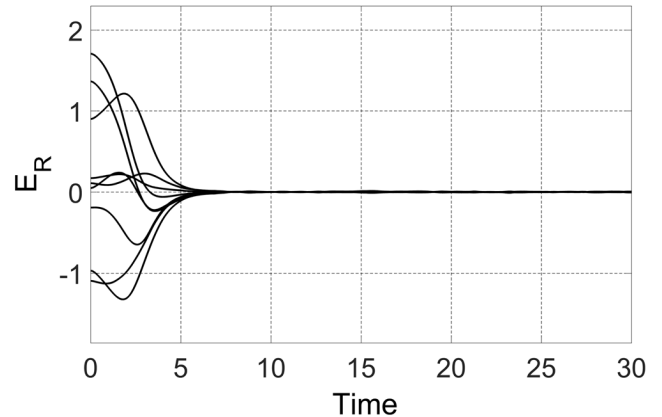


FIGURE 3. The trajectory of E_R with E_ω feedback only.

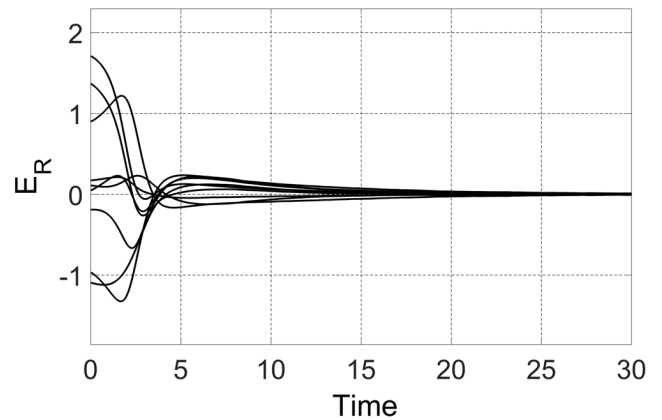


FIGURE 4. The trajectory of E_R with H_∞ design.

A. NOMINAL SYSTEM

Since A_c is time-invariant with all its eigenvalues residing in the open left complex plane, it is a well-known fact that the state of the nominal system (where d is assumed to be zero) will decay to zero exponentially. To see that, construct a quadratic Lyapunov function for (46) as

$$V = e^T Y e, \quad Y = Y^T > 0$$

where the constant symmetric positive definite matrix Y satisfies the following Lyapunov equation

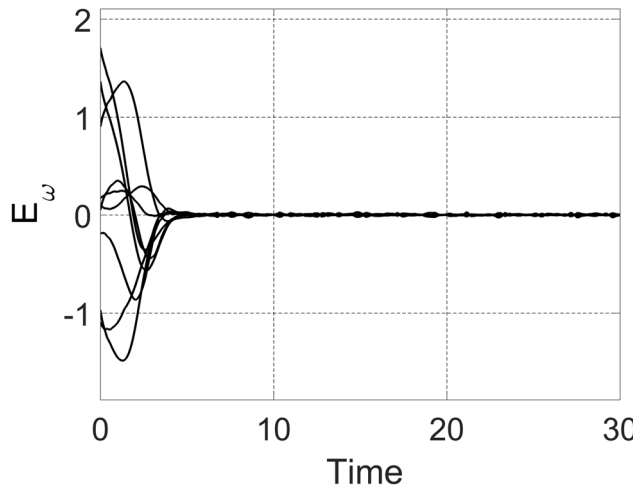
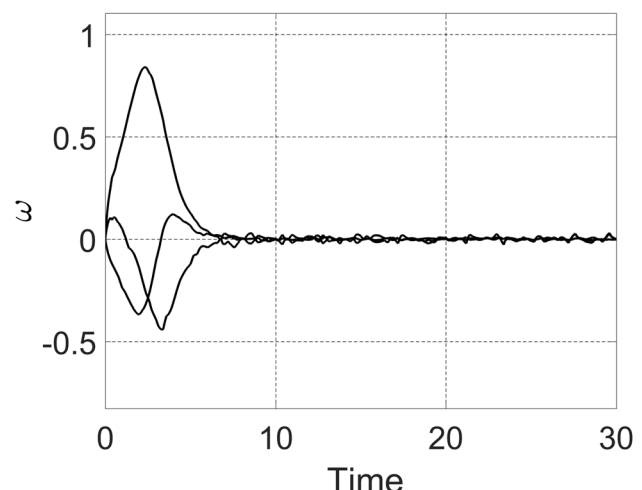
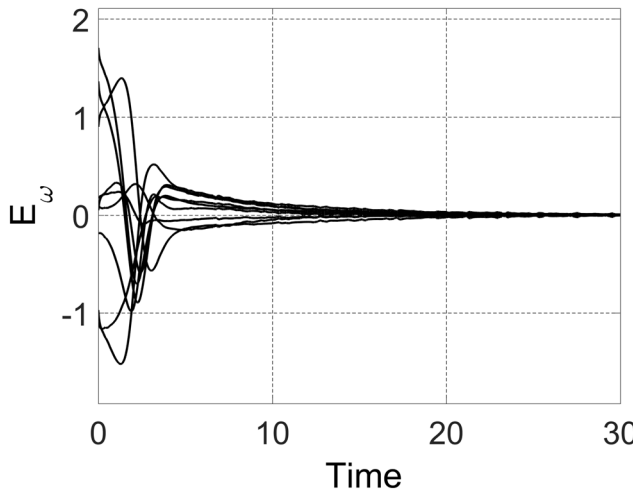
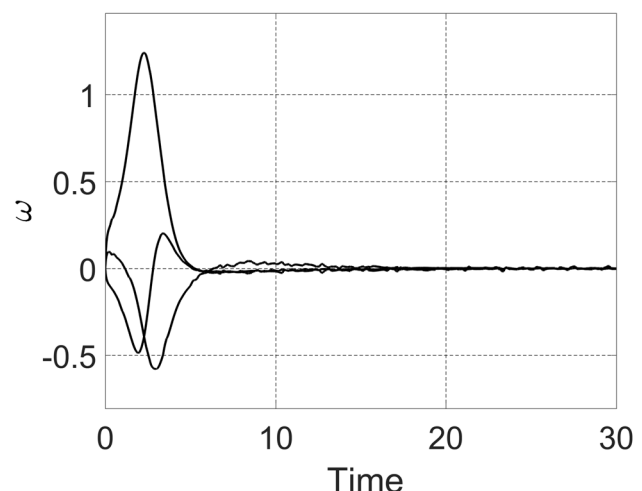
$$A_c^T Y + YA_c + I = 0. \quad (47)$$

Note that the eigenvalues of Y are real and positive, hence V is always positive when the error is non-zero. Consider the time-derivative of the Lyapunov function

$$\dot{V} = e^T (A_c^T Y + YA_c) e = -\|e\|^2 < 0, \quad \forall e \neq 0. \quad (48)$$

The Lyapunov function satisfies the following inequalities

$$\|e\|^2 \underline{\lambda}(Y) \leq V \leq \bar{\lambda}(Y) \|e\|^2. \quad (49)$$

**FIGURE 5.** The trajectory of E_ω with E_ω feedback only.**FIGURE 7.** The trajectory of ω with E_ω feedback only.**FIGURE 6.** The trajectory of E_ω with H_∞ design.**FIGURE 8.** The trajectory of ω with H_∞ design.

where $\underline{\lambda}(Y)$ and $\bar{\lambda}(Y)$ denote the minimum eigenvalue and maximum eigenvalue of Y , respectively. As a result

$$\dot{V} \leq -\frac{1}{\bar{\lambda}(Y)} V. \quad (50)$$

It can be concluded that the error dynamics of the nominal system is exponentially stable when the lumped disturbance and uncertainty d is assumed to be negligible.

B. NON-NOMINAL SYSTEM

In practice, external disturbance, system uncertainty, and sensor measurement errors and/or noises may not be negligible. Assume the lumped disturbance/uncertainty is bounded for all time and satisfies

$$\|d\| \leq \bar{d}, \quad (51)$$

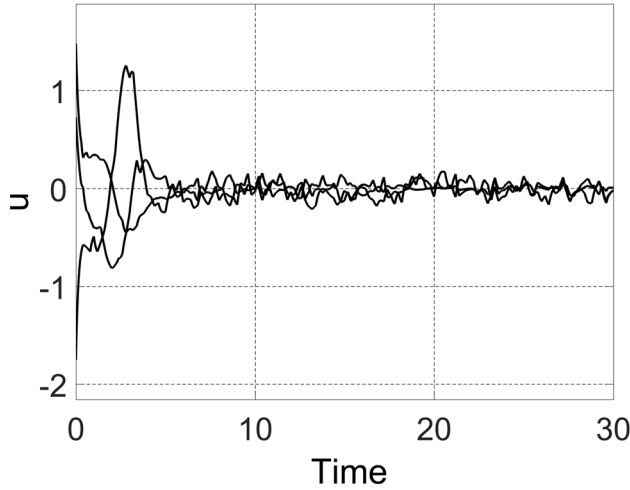
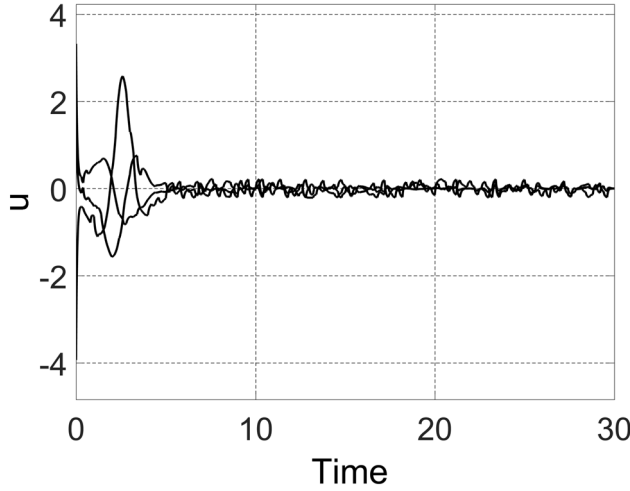
where \bar{d} is a constant representing the upper bound of the lumped disturbance/uncertainty. Consider (46)-(47) again.

The time-derivative of the Lyapunov function in this case becomes

$$\begin{aligned} \dot{V} &= e^T (A_c^T Y + YA_c) e + 2e^T Y B d \\ &\leq -\|e\|(\|e\| - 2\bar{d}\|Y\|). \end{aligned} \quad (52)$$

It can be concluded that after certain period of time, the magnitude of the error remains inside a ball with its radius equaling to $2\bar{d}\|Y\|$ and stays therein afterwards.

Apparently, the closed loop stability no longer belongs to the exponential type when the lumped disturbance/uncertain is not negligible. Unlike the robust control design presented in Section VI where the induced norm of the transfer function from the disturbance to the performance output is predetermined, the degree of robustness of the two controllers given in Section V for the nominal system cannot be specified in advance and cannot be guaranteed.

FIGURE 9. The trajectory of u with E_ω feedback only.FIGURE 10. The trajectory of the control u with H_∞ design.

VIII. VALIDATION AND PERFORMANCE ASSESSMENT

The proposed approach is validated *via* a numerical example in this section and two schemes are put to test for performance assessment. The difference between these two different schemes lies in the choice of the second control component f , that is, the specialized (nominal) non-robust scheme only utilizes E_ω whereas the robust scheme employs full error information in the H_∞ sense. Both of them, however, are subject to disturbances that are arbitrarily generated.

The initial attitude and the desired value are arbitrarily chosen. The initial angular velocity is set to zero for simplicity. Also given are the initial and desired roll, pitch, and yaw angles (denoted as ϕ , θ and ψ , respectively) and the corresponding rotation matrix that defines the attitude. For easy assessment, trajectories of the errors, the control signal u , the angular velocity ω , and the lumped disturbances are plotted. The disturbance attenuation level for the robust scheme is set to be $\gamma = 1.05$.

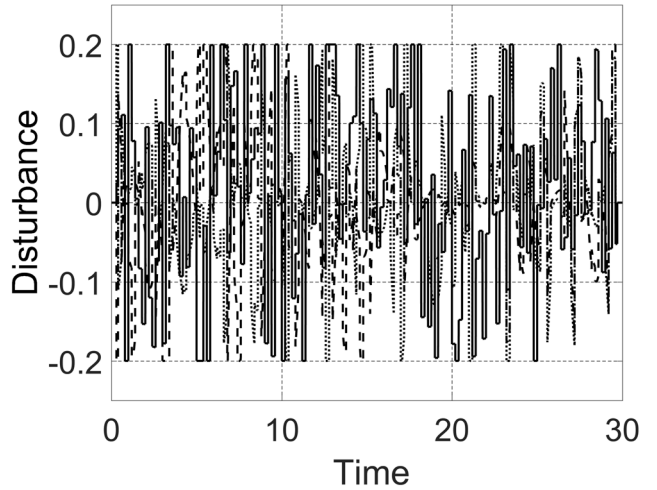


FIGURE 11. The trajectory of disturbances put into the system.

Example:

$$J = \begin{bmatrix} 1 & 0 & 0 \\ 0 & 1 & 0 \\ 0 & 0 & 3 \end{bmatrix}, \quad \begin{bmatrix} \phi(0) \\ \theta(0) \\ \psi(0) \end{bmatrix} = \begin{bmatrix} -80^\circ \\ -50^\circ \\ 20^\circ \end{bmatrix},$$

$$\begin{bmatrix} \phi_d \\ \theta_d \\ \psi_d \end{bmatrix} = \begin{bmatrix} 100^\circ \\ 70^\circ \\ 150^\circ \end{bmatrix},$$

$$R(0) = \begin{bmatrix} 0.1116 & 0.8799 & -0.4618 \\ -0.6330 & 0.4212 & 0.6495 \\ 0.7660 & 0.2198 & 0.6040 \end{bmatrix},$$

$$R_d = \begin{bmatrix} -0.0594 & 0.7713 & 0.6337 \\ 0.3368 & 0.6131 & -0.7146 \\ -0.9397 & 0.1710 & -0.2962 \end{bmatrix},$$

$$g_i = -0.0004, \quad g_p = 1,$$

Nominal design: $k_\omega = 5$,

Robust design: $k_i = 3.2733$, $k_p = -4.6626$, $k_\omega = 15.8696$.

Based on the above data, simulations are conducted to generate the trajectories of errors, angular velocities, controls, and the disturbance put into the system. See Fig. 2 – Fig. 10.

As demonstrated by these trajectory figures, both schemes worked well as all the undesired errors dropped to very small values rapidly, though noticeable disturbances were put into the system, and the initial attitude errors were chosen to be quite large purposefully. Even so, it should be pointed out that the capability of disturbance attenuation of the non-robust design cannot be guaranteed, *i.e.* lacking robustness against disturbance is its disadvantage compared to the robust counterpart.

IX. CONCLUSION

Under a unified SO(3) framework, the attitude control problem of quadrotor UAVs was studied and solved in this paper by a problem reformulation approach that renders it much more transparent to tackle. Virtual control and entry-wise

treatment of the governing differential matrix errors were utilized to further transform the problem into the stabilization of a 3-dimensional LTI system that was much easier to solve. A structurally simple and easy-to-implement design was presented. Furthermore, based on the classical H_∞ control theory, another robust design with certain capability of disturbance attenuation was also provided.

An example is provided to validate the proposed approach. Numerical simulations were conducted and the trajectories of errors and controls were also given that verified the effectiveness of the design and support our new method.

Future works include building a testbed to experimentally validate the approach and assess its performance. Extension of the proposed framework to incorporate sliding-mode control or the-like into the scheme to further enhance its disturbance rejection capability and to achieve finite-time convergence are challenges.

REFERENCES

- [1] C. Kyrikou, S. Timotheou, P. Kolios, T. Theocharides, and C. Panayiotou, "Drones: Augmenting our quality of life," *IEEE Potentials*, vol. 38, no. 1, pp. 30–36, Jan. 2019.
- [2] N. Chaturvedi, A. Sanyal, and N. McClamroch, "Rigid-body attitude control," *IEEE Control Syst. Mag.*, vol. 31, no. 3, pp. 30–51, Jun. 2011.
- [3] T. Lee, "Robust adaptive attitude tracking on $\text{SO}(3)$ with an application to a quadrotor UAV," *IEEE Trans. Control Syst. Technol.*, vol. 21, no. 5, pp. 1924–1930, Sep. 2013.
- [4] B. Zhao, B. Xian, Y. Zhang, and X. Zhang, "Nonlinear robust adaptive tracking control of a quadrotor UAV via immersion and invariance methodology," *IEEE Trans. Ind. Electron.*, vol. 62, no. 5, pp. 2891–2902, May 2015.
- [5] Y.-C. Choi and H.-S. Ahn, "Nonlinear control of quadrotor for point tracking: Actual implementation and experimental tests," *IEEE/ASME Trans. Mechatronics*, vol. 20, no. 3, pp. 1179–1192, Jun. 2015.
- [6] T. Lee, "Global exponential attitude tracking controls on $\text{SO}(3)$," *IEEE Trans. Autom. Control*, vol. 60, no. 10, pp. 2837–2842, Oct. 2015.
- [7] X.-N. Shi, Y.-A. Zhang, and D. Zhou, "Almost-global finite-time trajectory tracking control for quadrotors in the exponential coordinates," *IEEE Trans. Aerosp. Electron. Syst.*, vol. 53, no. 1, pp. 91–100, Feb. 2017.
- [8] B. Tian, L. Liu, H. Lu, Z. Zuo, Q. Zong, and Y. Zhang, "Multivariable finite time attitude control for quadrotor UAV: Theory and experimentation," *IEEE Trans. Ind. Electron.*, vol. 65, no. 3, pp. 2567–2577, Mar. 2018.
- [9] T. Jiang, D. Lin, and T. Song, "Finite-time backstepping control for quadrotors with disturbances and input constraints," *IEEE Access*, vol. 6, pp. 62037–62049, Nov. 2018.
- [10] S. Berkane, A. Abdessameud, and A. Tayebi, "Hybrid output feedback for attitude tracking on $\text{SO}(3)$," *IEEE Trans. Autom. Control*, vol. 63, no. 11, pp. 3956–3963, Nov. 2018.
- [11] A. K. Bhatia, J. Jiang, Z. Zhen, N. Ahmed, and A. Rohra, "Projection modification based robust adaptive backstepping control for multipurpose quadcopter UAV," *IEEE Access*, vol. 7, pp. 154121–154130, Nov. 2019.
- [12] O. Garcia, P. Ordaz, O.-J. Santos-Sanchez, S. Salazar, and R. Lozano, "Backstepping and robust control for a quadrotor in outdoors environments: An experimental approach," *IEEE Access*, vol. 7, pp. 40636–40648, Nov. 2019.
- [13] B. Tian, J. Cui, H. Lu, Z. Zuo, and Q. Zong, "Adaptive finite-time attitude tracking of quadrotors with experiments and comparisons," *IEEE Trans. Ind. Electron.*, vol. 66, no. 12, pp. 9428–9438, Dec. 2019.
- [14] A. Nikhilraj, H. Simha, and H. Priyadarshan, "Optimal energy trajectory generation for a quadrotor UAV using geometrically exact computations on $\text{SE}(3)$," *IEEE Control Syst. Lett.*, vol. 3, no. 1, pp. 216–221, Jan. 2019.
- [15] C. Izaguirre-Espinosa, A. J. Munoz-Vazquez, A. Sanchez-Orta, V. Parra-Vega, and I. Fantoni, "Fractional-order control for robust Position/Yaw tracking of quadrotors with experiments," *IEEE Trans. Control Syst. Technol.*, vol. 27, no. 4, pp. 1645–1650, Jul. 2019.
- [16] A. Akhtar and S. Waslander, "Controller class for rigid body tracking on $\text{SO}(3)$," *IEEE Trans. Autom. Control*, early access, Jul. 9, 2020, doi: 10.1109/TAC.2020.3008295.
- [17] H. Chu, Q. Jing, Z. Chang, Y. Shao, X. Zhang, and M. Mukherjee, "Quadrotor attitude control via feedforward all-coefficient adaptive theory," *IEEE Access*, vol. 8, pp. 116441–116453, Jul. 2020.
- [18] X. Tan, S. Berkane, and D. Dimarogonas, "Constrained attitude maneuvers on $\text{SO}(3)$: Rotation space sampling, planning and low-level control," *Automatica*, vol. 112, Feb. 2020, Art. no. 108659.
- [19] F. Lewis, D. Vrabie, and V. Syrmos, *Optimal Control*, 3rd ed. New York, NY, USA: Wiley, 2012, pp. 302–303.
- [20] M. Green, and D. Limebeer, *Linear Robust Control*, International ed. Upper Saddle River, NJ, USA: Prentice-Hall, 2012, pp. 235–236.
- [21] L. Wang, Z. Song, X. Liu, Z. Li, T. Fernando, and H. H. C. Iu, "Continuous finite-time integral sliding mode control for attitude stabilization," *IEEE Trans. Circuits Syst. II, Exp. Briefs*, vol. 67, no. 10, pp. 2084–2088, Oct. 2020.
- [22] H. Haimovich and H. De Battista, "Disturbance-tailored super-twisting algorithms: Properties and design framework," *Automatica*, vol. 101, pp. 318–329, Mar. 2019.
- [23] I. Nagesh and C. Edwards, "A multivariable super-twisting sliding mode approach," *Automatica*, vol. 50, no. 3, pp. 984–988, Mar. 2014.



JEN-TE YU was born in Hualien, Taiwan. He received the M.S. degree in aerospace engineering and electrical engineering from Wichita State University, USA, the M.S. degree in aerospace engineering and electrical engineering from the Georgia Institute of Technology, USA, and the Ph.D. degree in electrical engineering from National Taiwan University, Taiwan.

Since August 2016, he has been an Assistant Professor with the Department of Electrical Engineering, Chung Yuan Christian University (CYCU), Taiwan, where he currently serves as the Director for the Modern Control Laboratory. Prior to joining CYCU, he had worked in the industry for years in USA and Taiwan, as an Engineer and later as a Corporate Research and Development Manager. He has more than 30 publications in journals and conference proceedings, covering the areas of linear quadratic Gaussian (LQG) control over communication networks, model-free motion control, output feedback design of strictly positive real (SPR) systems, adaptive control, and optimal output feedback control. His recent research interests include networked control subject to sporadic packet dropout, linear quadratic regulator theory, consensus of multi-agent systems, and output feedback design of negative imaginary systems.